Author(s): Hänninen, Mikko M.; Baldansuren, Amgalanbaatar; Pugh, Thomas

Title: Structural and electronic elucidation of a N-heterocyclic silylene vanadocene adduct

Year: 2017

Version:

Please cite the original version:

Hänninen, M. M., Baldansuren, A., & Pugh, T. (2017). Structural and electronic elucidation of a N-heterocyclic silylene vanadocene adduct. Dalton Transactions, 46(30), 9740-9744. https://doi.org/10.1039/C7DT01226H

Journal Name

COMMUNICATION

Structural and electronic elucidation of a N-heterocyclic silylene vanadocene adduct

Mikko M. Hänninen*[a][b], Amgalanbaatar Baldansuren,[a] Thomas Pugh[a]

Received 00th January 20xx,
Accepted 00th January 20xx

DOI: 10.1039/x0xx00000x

www.rsc.org/

The solid and solution state structure of the vanadium(II) N-heterocyclic silylene (NHSi) complex, [(^{Si}IPr)V(Cp)$_2$] (1) is reported (^{Si}IPr: 1,3-bis(2,6-diisopropylphenyl)-1,3-diaza-2-silacyclopent-4-en-2-ylidene). The electronic structure of 1 is probed using combination of magnetic measurements, EPR spectroscopy and computational studies. The V–Si bond strength and complex forming mechanism between vanadocene and NHSi ligand is elucidated using computational methods.

Vanadocene, [V(C_5H_5)$_2$], is one of the few stable early transition metal metallocenes that exists in traditional sandwich structure. It is a coordinatively and electronically unsaturated molecule with intriguing reactivity, such as oxidative addition of unsaturated hydrocarbons or nitriles and cyclopentadienyl displacement reactions.[1-5] Unlike many other first-row metallocenes,[6-8] vanadocene has no structurally characterized complexes with N-heterocyclic carbenes (NHCs) or heavier low-valent group 14 homologues.

Recently, we have shown that N-heterocyclic silylene (NHSi)[9-11] ligands can form complexes analogous to N-heterocyclic carbenes with Fe(N'')$_2$ (N'' = bis(trimethylsilyl)amide) and that the NHSi coordination compounds are stabilized by the back-bonding and dispersion forces.[12] From these results, it is perceivable that by enhancing the back-bonding ability of the metal cation, stable silylene complexes could be prepared even in the absence of significant dispersion stabilization. Vanadocene fulfils both above mentioned requirements as low-valent vanadium(II) should be able to participate to back-bonding whereas cyclopentadienyl ligands lack suitable sp^3 hybridized C–H moieties commonly observed in dispersion stabilized molecules.[13]

Even though NHSi's are isostructural with NHCs, the electronic structures of such compounds are drastically different. While NHCs are generally strong σ-donors, their π-acceptor ability is strongly dependent on the heterocyclic substituents. Divalent NHSi's on the other hand, can be seen as π-acceptors with reduced σ-donor character.[14]

We began our investigation by attempting the synthesis of NHC complex [(IPr)V(Cp)$_2$] (IPr: 1,3-bis(2,6-diisopropylphenyl)imidazol-2-ylidene). Unfortunately, all efforts to isolate this species were unsuccessful (Scheme 1). The combination of electron rich metal cation and poor π-accepting capabilities of standard NHCs was hypothesized to preclude the formation of a stable complex.

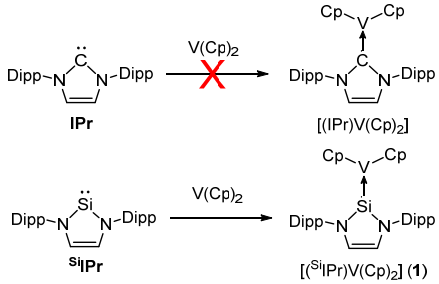

Scheme 1. Attempted complexation reactions. Dipp = 2,6-diisopropylphenyl.

Because of the enhanced π-accepting ability of silylene ligands,[12] we synthesized a vanadocene-silylene adduct. Upon dissolving V(Cp)$_2$ and ^{Si}IPr in hexane at -78°C, a dark red solution was obtained. The colour of the solution remained unchanged when warmed to room temperature. Upon cooling a concentrated solution to -30 °C over 24 hours, dark red-black crystals were formed in 71% yield. X-ray crystallography (Figure 1) confirmed the formation of [(^{Si}IPr)V(Cp)$_2$] (**1**). In the solid-state, the ^{Si}IPr ligand is coordinated to vanadium with V–Si bond length of 2.358 Å (average of two molecules in the asymmetric unit). V–Cp$_{cent}$ distances are between 1.902 and 1.907 Å which are slightly (0.01 Å) shorter compared to free V(Cp)$_2$. The cyclopentadienyl ligands are bent with an average Cp–V–Cp angle of 146.1 degrees for the two molecules.

[a] School of Chemistry, The University of Manchester
Oxford Road, Manchester, M13 9PL UK.
[b] Department of Chemistry, University of Jyväskylä
P.O. Box 35, FI-40014, Jyväskylä, Finland

Information (ESI) available: Experimental and computational details, additional characterization data, *xyz*-coordinates of the geometry optimized compounds.
See DOI: 10.1039/x0xx00000x

The ^{1}H NMR spectrum of **1** in benzene-D_6 at 298 K shows relatively sharp signals that are shifted only slightly with respect to non-coordinated ^{Si}IPr. The isopropyl methyl protons resonate at 1.22 and 1.28 ppm, and the associated methine protons occur as a broad peak at 3.29 ppm. The signals for the Dipp aromatic protons are in the range 7.15-7.23 ppm, and the silylene backbone protons occur as a broad singlet at 6.46 ppm. In addition, the ^{1}H NMR spectrum at 298 K contains several paramagnetically shifted signals. Largest shift occurs at about 320 ppm, which is close to the $V(Cp)_2$ resonance.[15] Four broad, more notably shifted signals compared to free ligand resonances are observed at 0.14, 3.57, 6.88 and 7.65 ppm. These features suggest a coordination equilibrium in solution *i.e.* ^{Si}IPr ligand coordinates and dissociates from the metal fragment but at slower rate than the NMR experiment time scale hence two sets of signals are present.

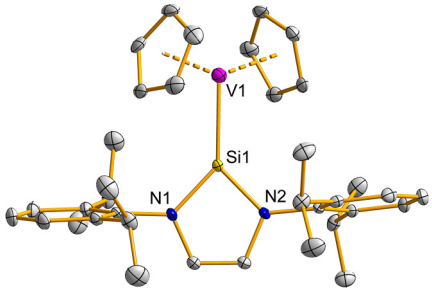

Figure 1. Solid state structure of 1. Thermal ellipsoids have been drawn at 30 % probability and hydrogen atoms are omitted for clarity. Selected bond distances (Å) and angles (°) as an average of the two molecules of the asymmetric unit: V1–Si1 2.3581, V1–Cp 1.908 and 1.904, Si1–N1 1.761, Si1–N2 1.762; Cp(1)–V1C–Cp(2) 146.0, N1–Si1–N2 88.1.

This behaviour was further investigated with variable temperature NMR spectroscopy in the temperature range from 238 to 328 K (Figure 2). The broad resonances observed at room temperature intensify upon cooling while the sharp signals of ^{Si}IPr ligand disappear almost completely at 238 K. Furthermore, the extremely broad peak at 318 ppm assigned to free $V(Cp)_2$ diminishes. VT-NMR indicates that in lower temperatures silylene ligand is indeed completely coordinated to vanadocene but at higher temperatures ^{Si}IPr becomes reasonably labile.

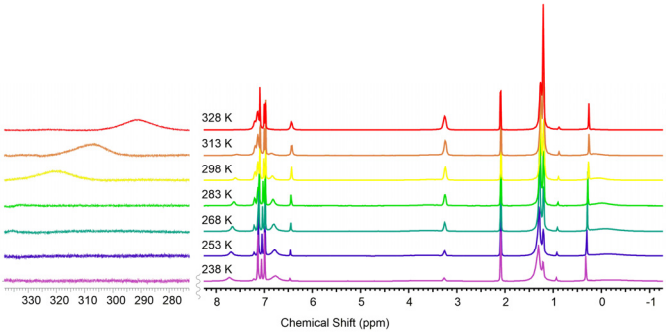

Figure 2. ^{1}H NMR spectrum of **1** in temperature range 238-333 K in toluene-D_8.

The UV-VIS-NIR spectrum of **1** in hexane shows four distinct absorptions at 283, 405, 565 and 1473 nm (Figure S3). The first four signals are likely from metal-to-ligand excitations while the lowest energy peak is assigned to *d-d* transition. This interpretation is supported by the calculated spectrum (Figure S4) showing strongest transitions at 275, 366 and 551 nm. The signal from the vanadium d-d- transition is calculated to be around 1020 nm, which is in qualitative agreement with the experiment. It should be noted that the fluxional coordination in solution would have major effect on this kind of transitions which explains the rather large difference between the calculated and observed value.

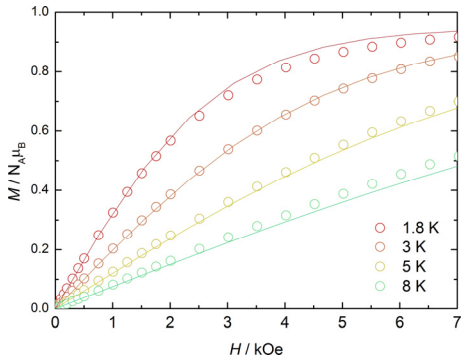

Figure 3. The field (*H*) dependence of magnetization (*M*) at different temperatures.

The magnetic susceptibility of a polycrystalline sample of **1** restrained in eicosane, was measured in the temperature range 2-300 K (Figure S5) and the field dependence of magnetization at 1.8, 3, 5 and 8 K (Figure 3). The value of $\chi_M T$ at 300 K is 0.41 cm^3 K mol^{-1}, with very little variation down to approximately 70 K. At lower temperatures, $\chi_M T$ decreases before experiencing a steep drop below 40 K which is most likely due to depopulation of low lying excited states. A value of 0.32 cm^3 K mol^{-1} is reached at 2 K. The susceptibility and magnetization data were both fitted using PHI[16] with S = 1/2 and isotropic *g*-value of 1.9; modelling using anisotropic g-tensor parameters did not improve the fit.

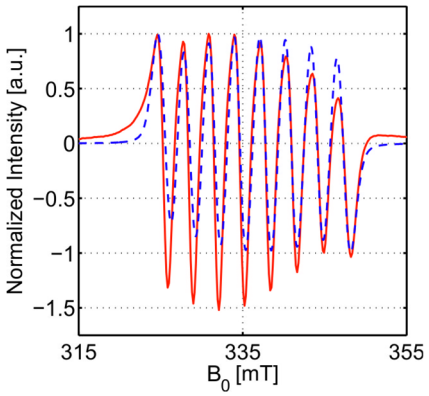

Figure 4. X-band continuous wave EPR spectrum of vanadium-silylene (fluid solution de-gassed and sealed in a tube) measured at room temperature (~ 298 K), and its corresponding numerical simulation. The simulation takes into account the natural abundance of ^{51}V (I = 7/2) nucleus and the isotropic hyperfine coupling between S = ½ and I = 7/2 of ^{51}V nucleus in solution.

Electron paramagnetic resonance (EPR) studies were performed to obtain more information about the electronic structure of **1**. Figure 4 shows the isotropic spectrum of vanadium-silylene complex in hexane solution with its corresponding numerical simulation. The *g*-value is orientationally averaged out, and only its isotropic value $g_{iso} = (g_{||} + 2g_{\perp})/3 \sim 1.995$ has been measured at room temperature. In addition, g_{iso} is smaller than a free electron *g*-value,

indicating that the unpaired electron for a low-spin S=1/2 state originates from a less than half-filled *d* shell of transition metal ion.[17] In a similar way, only the isotropic value for hyperfine coupling can be measured in solution at room temperature. In Figure 4, the well-resolved spectrum is assigned to the isotropic hyperfine splitting, $A_{iso} = (A_{||} + 2A_{\perp})/3 \sim 3.1$ mT (87 MHz), of vanadium ion in solution. The experimental $A_{iso} = 87$ MHz is to be compared with an average atomic value of 4165 MHz of ^{51}V,[18] and the 4*s* orbital contribution to the spin density distribution is just about 2.1%.

At lower temperatures, the complex still exists in the low-spin ($S = 1/2$) state. At 10 K, the EPR spectrum (Figure S6 in ESI) significantly differs from the anisotropic splitting of a high-spin ($S = 3/2$ from $3d^3$) complex in frozen solution.[19] In our case, neither the g-anisotropy nor the hyperfine anisotropy was completely resolved at X-band. Our initial hypothesis was that only the permissible transition ($\Delta M_I = 0$) between $m_I = -1/2$ and $m_I = +1/2$ nuclear sublevels was resolved in the parallel ($g_{||}$) region at 334 mT as there were no resonant transitions in the perpendicular ($g_{\perp}$) region at 167 mT. However, interactions between neighbouring paramagnetic centres cannot be ruled out completely. The features of the observed spectra could also be assigned to non-dilute system in which the magnetic dipole-dipole interaction between paramagnetic neighbours should broaden the line. There are isotropic and anisotropic exchange interactions between spins of the two neighbouring electrons, the exchange integral (*J*) is dependent upon overlap of the wave functions and it falls off very rapidly as the distance between ions is increased. The isotropic value ($J = 84$ MHz) was deduced from the numerical simulation (Figure S6) and this empirical parameter resulted in rather good agreement with the experimental spectrum.

A computational study was performed to shed light to the electronic structure and bonding in **1**. Geometry optimization of [(^{Si}IPr)V(Cp)$_2$] at PBE0/Def2mix level (Def2-TZVP basis set for the vanadium and silicon atoms and the Def2-SVP basis set for all other atoms) leads to a stable species with both feasible spin states (S = 1/2 and S = 3/2, **1-LS** and **1-HS**, respectively). As suggested by the EPR and magnetic studies, the doublet is the electronic ground state by about 10 kcal/mol. The geometrical parameters obtained from the optimization for **1-LS** are also in very good agreement with the experiment (Table 1). The largest differences in bond lengths are less than 0.03 Å and the most important bond angles differ only about 1° from the solid-state structure.

Unlike ^{Si}IPr, vanadocene and IPr do not form a stable high spin (S = 3/2) complex, and during the geometry optimization the IPr ligand completely detaches from the vanadium(II) center. However, optimization of the low-spin system yields a stable compound with a V–C bond length of 2.231 Å. Hence, it is somewhat surprising that we were not able to isolate [(IPr)V(Cp)$_2$] experimentally considering that doublet is the electronic ground state of the silylene complex.

The reason for this behavior is suspected to lie behind the intrinsic differences of ^{Si}IPr and IPr ligands. For [(^{Si}IPr)V(Cp)$_2$] following bond forming mechanism can be conceived; ^{Si}IPr ligand coordinates weakly to high spin V(Cp)$_2$ donating electron density from both σ- and π-symmetric molecular orbitals to unoccupied d orbitals of V(II) cation, initially binding the ligand to the metal center. The steric repulsion will force the Cp rings to bend away from the silylene ligand thus breaking the overall symmetry of the vanadocene and altering the d orbital energies. It is known that electronic ground state of metallocenes can change upon bending the cyclopentadienyl ligands.[20, 21] However, it is important to notice, that in **1** (solid state geometry) the bent vanadocene fragment alone is still a high spin (quartet) system by about 16 kcal/mol.

Table 1. Comparison of selected geometrical parameters to experimentally observed.

		1-HS		**1-LS**	
	Exp$_{avg}$	S = 3/2	Δ[a]	S = 1/2	Δ[a]
V1–Si1	2.3581	2.4576	0.0995	2.3305	0.0276
V1–Cp1	1.908	2.095	0.188	1.890	0.018
V1–Cp1	1.904	2.080	0.176	1.892	0.012
Si1–N1	1.761	1.749	0.011	1.765	0.004
Si1–N2	1.762	1.749	0.015	1.766	0.004
Cp1–V1–Cp2	146.0	130.7	15.3	147.2	1.2
N1–Si1–N2	88.1	88.5	0.5	89.0	0.1

[a] Δ = Absolute difference to the experimental value.

Since the lowest unoccupied molecular orbital (LUMO) of ^{Si}IPr is a diffuse π-symmetric orbital, back-donation will stabilize the donating metal d orbital. This increases the orbital splitting eventually overcoming the electron pairing energy and facilitating the lower overall spin state (*i.e.* double occupation of one metal d orbital). Double occupation also vacates low lying d orbital to accept electron donation from the ligand further strengthening the dative bond.

A similar process is not feasible for traditional NHCs since their empty π-type orbital lies higher in energy and is not as readily available for back-bonding. In addition, IPr is a worse π-donor than ^{Si}IPr, which also hinders the formation of initial quartet state complex. For these reasons, the low-spin state will not be achieved and [(IPr)V(Cp)$_2$] cannot be isolated experimentally. Hence, only binding of a suitable ligand like silylene or carbonyl[22] to V(Cp)$_2$ fragment will stabilize the low spin system thus enabling the preparation of [(^{Si}IPr)V(Cp)$_2$].

It should be also noted that even though the formation of vanadacyclopropenes through oxidative addition of alkynes is a well-known reaction,[1, 23-25] the calculated electronic structure and observed V–Si and Si–N bond distances suggest that both vanadium and silylene remain at their original formal oxidation state of +2.

Further information about the V–E (E = C or Si) bond can be extracted from the bond dissociation energies (BDE). Calculated BDE for **1-LS** breaking into ^{Si}IPr and low spin V(Cp)$_2$ is 39.5 kcal/mol while corresponding value for [(IPr)V(Cp)$_2$] is 27.0 kcal/mol. These values only describe the bond strength without relaxation of V(Cp)$_2$ to its quartet ground state. With this considered, BDE values of -0.1 and -12.6 kcal/mol are obtained for **1-LS** and [(IPr)V(Cp)$_2$], respectively. This indicates that the initial formation of **1-HS** is only kinetically stabilized but also that at high spin state, the V(Cp)$_2$–IPr interaction is

repulsive further elucidating why [(IPr)V(Cp)$_2$] cannot be experimentally isolated.

Energy decomposition analysis (EDA) is a quantitative method to study chemical bonds by dividing the (instantaneous) interaction energy (ΔE_{int}) between two fragments into three distinct terms that can be used to describe the nature and strength of a chemical bond.[26] The terms are ΔE_{elstat}, describing the quasiclassical electrostatic interaction, ΔE_{Pauli} that takes into account the repulsive exchange interaction between same spin electrons of the two fragments, and an orbital interaction term, ΔE_{orb}, arising from the mixing and relaxation of the fragment orbitals when the two fragments are brought together. ΔE_{orb} can be broadly viewed as the covalent contribution of the bond.

The EDA was utilized to study the bonding in complex **1** and hypothetical [(IPr)V(Cp)$_2$] (Table 2). As can be expected for neutral IPr and ^{Si}IPr ligands, regardless the electronic ground state, the orbital interaction term makes a significant contribution to ΔE_{int}. The repulsive exchange interactions completely compensate the attractive electrostatic terms, resulting in sizable steric repulsions (steric = ΔE_{elstat} + ΔE_{Pauli}) between the fragments. The interaction energy in **1-LS** is almost 20 kcal/mol higher compared to the **1-HS** which is expected considering the bond formation mechanism described above. The ΔE_{int} in doublet state [(IPr)V(Cp)$_2$] is reasonably large but because the lack of low-lying π-symmetric orbital capable for back-bonding, the NHC ligand cannot facilitate the spin transition of V(Cp)$_2$ fragment hence [(IPr)V(Cp)$_2$] is not experimentally observed.

Table 2. Selected results from the EDA analysis (in kcal/mol).

	E_{int}	E_{orb}	Steric	E_{Pauli}	E_{elstat}
[(^{Si}IPr)V(Cp)$_2$], **1-LS**	-50.01	-83.59	33.57	143.3	-109.72
[(^{Si}IPr)V(Cp)$_2$], **1-HS**	-33.20	-107.99	74.78	234.42	-157.64
[(IPr)V(Cp)$_2$], (S = 1/2)	-47.04	-58.11	11.08	110.32	-99.25

Extended Transition State – Natural Orbitals for Chemical Valence (ETS-NOCV) approach can be used to partition the charge and energy of a chemical bond into the different components (σ, π, δ).[27] ETS-NOCV gives the energy contributions for each specific (orbital) interaction between fragments hence it can be utilized for example to study donation and back-donation in metal-ligand bonds. The NOCV deformation densities, Δρ, depicted in Figure 5 shows the electron density transfer between different NOCV orbitals. The two main (orbital derived) bonding contribution comes from the σ-donation (-35.7 kcal/mol) from the silylene ligand to empty metal d orbital whereas π-back-donation from doubly occupied d orbital is responsible for about -30 kcal/mol of the total ETS-NOCV binding energy of -83.7 kcal/mol.

Insight to the bond order between vanadium and silicon/carbon was obtained by calculation of Wiberg bond indices (WBI). The calculated WBIs for low spin [(^{Si}IPr)V(Cp)$_2$] and [(IPr)V(Cp)$_2$] are 0.90 and 0.63, respectively. These values support the preceding computational analyses suggesting a (dative) single bond between V and Si but also corroborate the hypothesis of weaker NHC–vanadocene interaction. Furthermore, Driess *et al.* recently reported *s*-block complexes with related NHSi ((1,3-tert-butyl)-1,3-diaza-2-silacyclopent-4-en-2-ylidene) with Ae–Si (Ae = Ca, Sr, Ba) WBIs around 0.5.[28, 29] The smaller values could be explained by the lack of back-bonding interactions between the Ae and NHSi hence agreeing with our bonding analysis.

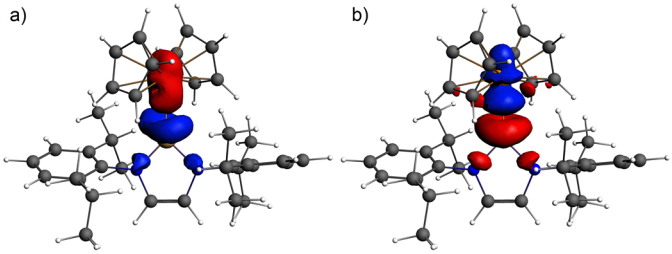

Figure 5. The two largest contribution to NOCV deformation densities (Δρ) in **1** (red Δρ < 0; blue Δρ > 0). (a) Si-to-V σ-donation; -35.7 kcal/mol. (b) V-to-Si π-donation; 30.1 kcal/mol.

In conclusion, we have prepared and fully characterized the first vanadocene complex of an NHSi ligand. Furthermore, [(^{Si}IPr)V(Cp)$_2$] adds to the very small collection of group 4 and 5 metal complexes with any silylene ligands.[30] The ^{Si}IPr ligand is firmly bound to vanadium(II) cation in solid state whereas coordination is dynamic in solution at room temperature. VT-NMR spectroscopy experiments suggest that at 238 K silylene ligand is more tightly bound to vanadocene. Coordination of π-accepting ^{Si}IPr stabilizes the low-spin ground state of the vanadium center rendering it suitable for σ-donation, which enables V–Si bond formation and isolation of **1.** In contrast, the poor π-acceptor properties of IPr inhibit the formation of [(IPr)V(Cp)$_2$]. Furthermore, EDA and NOCV analyses confirm that the V–Si bond is stabilized by the π-back-bonding from doubly occupied metal d orbital to the lowest unoccupied orbital of ^{Si}IPr, corroborating the presented bond formation mechanism.

Acknowledgements

The guidance and support from Prof. Richard A. Layfield during MH's research visit at The University of Manchester is greatly appreciated. We thank the EPSRC UK National EPR Research Facility and Service at the University of Manchester for support with EPR measurements. We also thank *CSC – IT Center for Science* for computational resources and Dr J. Mikko Rautiainen for fruitful discussions during the preparation of the manuscript. MH is grateful to Academy of Finland (grant number 274505) for funding.

Notes and references

1 R. Choukroun and C. Lorber, *Eur. J. Inorg. Chem.*, 2005, 4683-4692.

2 C. Fernández-Cortabitarte, F. García, J. V. Morey, M. McPartlin, S. Singh, A. E. H. Wheatley and D. S. Wright, *Angew. Chem. Int. Ed.*, 2007, **46**, 5425-5427.

3 N. L. Ermolaev and V. K. Cherkasov, *Russ. Chem. Bull.*, 2013, **61**, 1550-1552.
4 F. A. Stokes, M. A. Vincent, I. H. Hillier, T. K. Ronson, A. Steiner, A. E. H. Wheatley, P. T. Wood and D. S. Wright, *Dalton Trans.*, 2013, **42**, 13923-13930.
5 F. A. Stokes, L. Kloo, Y. Lv, P. J. Harford, A. E. H. Wheatley and D. S. Wright, *Chem. Commun.*, 2012, **48**, 11298-11300.
6 C. D. Abernethy, J. A. C. Clyburne, A. H. Cowley and R. A. Jones, *JACS*, 1999, **121**, 2329-2330.
7 M. D. Walter, D. Baabe, M. Freytag and P. G. Jones, *Z. Anorg. Allg. Chem.*, 2016, **642**, 1259-1263.
8 M. Manßen, C. Adler and R. Beckhaus, *Chem. Eur. J.*, 2016, **22**, 4405-4407.
9 M. Denk, R. Lennon, R. Hayashi, R. West, A. V. Belyakov, H. P. Verne, A. Haaland, M. Wagner and N. Metzler, *JACS*, 1994, **116**, 2691-2692.
10 M. Haaf, T. A. Schmedake and R. West, *Acc. Chem. Res.*, 2000, **33**, 704-714.
11 M. Denk, J. C. Green, N. Metzler and M. Wagner, *J. Chem. Soc., Dalton Trans.*, 1994, 2405-2410.
12 M. M. Hanninen, K. Pal, B. M. Day, T. Pugh and R. A. Layfield, *Dalton Trans.*, 2016, **45**, 11301-11305.
13 D. J. Liptrot and P. P. Power, *Nature Reviews Chemistry*, 2017, **1**, 0004.
14 Z. Benedek and T. Szilvasi, *RSC Advances*, 2015, **5**, 5077-5086.
15 H. Eicher, F. H. Köhler and R. d. Cao, *The Journal of Chemical Physics*, 1987, **86**, 1829-1835.
16 N. F. Chilton, R. P. Anderson, L. D. Turner, A. Soncini and K. S. Murray, *J. Comput. Chem.*, 2013, **34**, 1164-1175.
17 K. Dyrek and M. Che, *Chem. Rev.*, 1997, **97**, 305-332.
18 J. R. Morton and K. F. Preston, *Journal of Magnetic Resonance (1969)*, 1978, **30**, 577-582.
19 T. A. Jackson, J. Krzystek, A. Ozarowski, G. B. Wijeratne, B. F. Wicker, D. J. Mindiola and J. Telser, *Organometallics*, 2012, **31**, 8265-8274.
20 J. W. Lauher and R. Hoffmann, *JACS*, 1976, **98**, 1729-1742.
21 J. C. Green, *Chem. Soc. Rev.*, 1998, **27**, 263-272.
22 S. Gambarotta, C. Floriani, A. Chiesi-Villa and C. Guastini, *Inorg. Chem.*, 1984, **23**, 1739-1747.
23 G. Fachinetti, C. Floriani, A. Chiesi-Villa and C. Guastini, *Inorg. Chem.*, 1979, **18**, 2282-2287.
24 J. L. Petersen and L. Griffith, *Inorg. Chem.*, 1980, **19**, 1852-1858.
25 M. Jordan, W. Saak, D. Haase and R. Beckhaus, *Organometallics*, 2010, **29**, 5859-5870.
26 T. Ziegler and A. Rauk, *Theor. Chim. Acta*, 1977, **46**, 1-10.
27 M. P. Mitoraj, A. Michalak and T. Ziegler, *J. Chem. Theory Comput.*, 2009, **5**, 962-975.
28 B. Blom, G. Klatt, D. Gallego, G. Tan and M. Driess, *Dalton Trans.*, 2015, **44**, 639-644.
29 B. Blom, A. Said, T. Szilvási, P. W. Menezes, G. Tan, J. Baumgartner and M. Driess, *Inorg. Chem.*, 2015, **54**, 8840-8848.
30 B. Blom, M. Stoelzel and M. Driess, *Chem. Eur. J.*, 2013, **19**, 40-62.